

Alkyl and aryl complexes of platinum(II) and palladium(II) containing the tri(1-cyclohepta-2,4,6-trienyl)phosphane ligand. Intramolecular dynamics and signs of coupling constants

Max Herberhold*, Thomas Schmalz, Wolfgang Milius, Bernd Wrackmeyer*

Laboratorium für Anorganische Chemie, Universität Bayreuth, D-95440 Bayreuth, Germany

Received 17 May 2002; accepted 28 August 2002

Dedicated to Prof. Martin A. Bennett

Abstract

Tri(1-cyclohepta-2,4,6-trienyl)phosphane, $P(C_7H_7)_3$ ([P] when coordinated to the metal centre), behaves as a bidentate chelating ligand in platinum(II) and palladium(II) complexes, $[P]MR_2$ [$M = Pt$, $R = Me$ (**3a**), Et (**3b**), Pr (**3c**), Bu (**3d**), CH_2Ph (**3e**), Ph (**3f**), C_6H_4-4-F (**3g**), C_6F_5 (**3h**), Fc (**3i**); $M = Pd$, $R = Me$ (**4a**), C_6F_5 (**4h**)], which were synthesized by the reaction of $[P]MCl_2$ with either LiR or $RMgBr$. The molecular structure of **3g** was determined by X-ray analysis, confirming the Pt–P bond and the η^2 -coordination of one of the C_7H_7 rings by its central C=C bond. In solution at room temperature, all complexes are fluxional with respect to the NMR time scale, due to intramolecular exchange of the C_7H_7 rings in η^2 -C=C coordination to the metal centre. The products were characterised by 1H , ^{13}C , ^{31}P and ^{195}Pt NMR spectroscopy, and signs of various coupling constants were determined by application of appropriate 1D spin tickling experiments and 2D heteronuclear shift correlations.

© 2003 Elsevier Science B.V. All rights reserved.

Keywords: Platinum; Palladium; Phosphanes; NMR; Coupling signs; X-ray

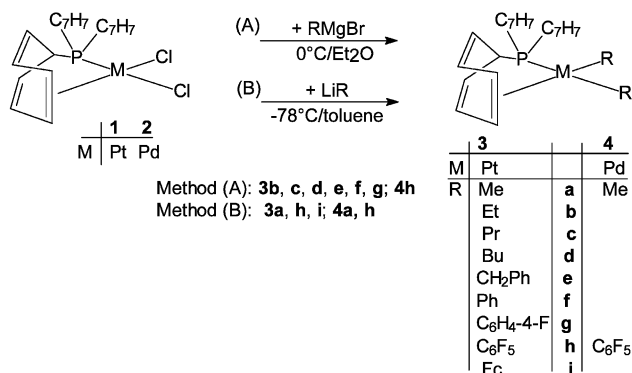
1. Introduction

Numerous bis(phosphane)platinum(II) and palladium(II) complexes bearing either alkyl or aryl groups in *cis* or *trans* positions are known [1]. Similarly, various (cod)Pt and (cod)Pd complexes (cod = cycloocta-1,5-diene) have been prepared [2]. However, complexes in which a phosphane and an η^2 -coordinated olefin simultaneously act as ligands in addition to alkyl and

aryl groups are rare [3,4]. Such complexes may be model compounds with respect to catalytic processes, in which an olefin becomes coordinated to the metal centre, reacts and is replaced by another olefin. We have shown that tri(1-cyclohepta-2,4,6-trienyl)phosphane, $P(C_7H_7)_3$ [5] (or [P] when coordinated to a metal), can act as a bidentate ligand in complexes of Pt(II) and Pd(II) through P–M and (η^2 -C=C)–M coordination of the central C=C bond of one of the C_7H_7 rings [6–11]. In particular the chlorides, $[P]MCl_2$ with $M = Pt$ (**1**) and Pd (**2**) [6], have served as useful starting materials in this chemistry. Recently, we have studied complexes of the type $[P]Pt(C\equiv C-R)_2$ by multinuclear magnetic resonance (1H , ^{13}C , ^{31}P , ^{195}Pt NMR) in order to explore the mutual influence of alkynyl groups upon the

* Corresponding author. Tel.: +49-921-55 2540; fax: +49-921-55 2157.

E-mail addresses: max.herberhold@uni-bayreuth.de (M. Herberhold), b.wrack@uni-bayreuth.de (B. Wrackmeyer).



Scheme 1.

respective functions in *trans* positions [11]. The present study focuses on the corresponding influence exerted by alkyl and aryl groups in [P]MR₂ complexes (see Scheme 1).

2. Results and discussion

2.1. Synthesis

As shown in Scheme 1, the platinum and palladium complexes **3** and **4** bearing various alkyl or aryl groups at the metal can be prepared by treatment of the chloride **1** or **2** with the respective organolithium or Grignard reagent. They are yellow (**3a–g**), bright-brown (**4a**), colourless (**3h, 4h**) or red solids (**3i**) which are moderately air-stable and can be stored for prolonged time without decomposition under argon atmosphere. Although numerous attempts were made to obtain single crystals, the compounds were always isolated as powders or microcrystalline materials, except of **3g**, of which single crystals suitable for X-ray structural analysis could be obtained (vide infra).

2.2. NMR spectroscopic measurements

The ¹³C, ³¹P and ¹⁹⁵Pt NMR data are given in the Tables 1 and 2, and ¹H NMR data are listed in the Section 4 (except of **3h** and **4h** in Table 2). The data confirm the proposed structures of **3** and **4** in solution, and they show that all complexes are fluxional with respect to η²-coordination of the central C=C bond of the three C₇H₇ rings. Fluxional behaviour has been observed for the coordination of other olefinic phosphanes **3c**[12].

2.2.1. Intramolecular dynamics

In the process of this intramolecular exchange, the groups in *cis*- and *trans*-positions relative to phosphorus do not exchange. This excludes a simple dissociative mechanism for C₇H₇ ring exchange, since in an inter-

mediate with regular three-coordinate M the two organyl groups at M would become identical. Similarly, there is no evidence for an associative mechanism involving a long-lived intermediate containing the metal in square-pyramidal surroundings. Such an intermediate with five-coordinate M should have the M at some stage in trigonal-bipyramidal surroundings which, again, would make the organyl groups indistinguishable. Therefore, it is suggested that the C₇H₇ ring exchange proceeds via a transition state, in which the outgoing ring is immediately replaced by an incoming ring. This mechanism appears to be general for all compounds of the type [P]M(L)(L') studied, as has been found previously [6–11]. Examples of square planar Rh(I), Pd(II) and Pt(II) complexes with other ligands have been reported with similar dynamic properties [13,14]. In Fig. 1A, the ¹H NMR spectrum of [P]PtMe₂ **3c** is shown as a typical example illustrating the dynamic behaviour (ΔG*(260 K) = 48 ± 2 kJ mol⁻¹). The rate of this dynamic process is dependent on the metal (Pt complexes are less dynamic than Pd complexes) and on the nature of the organyl groups. Fig. 2 shows the ¹H and ¹³C NMR spectra of [P]Pt(C₆F₅)₂ **3c**, where a rigid structure, with respect to the NMR time scale, appears to be present already at room temperature (in contrast to the analogous Pd complex **4h**).

2.2.2. Chemical shifts and coupling constants

The chemical shifts δ¹H, δ¹³C, and δ¹⁹⁵Pt are in the expected range. Interestingly, the differences in the δ³¹P values between Pt and Pd complexes do not follow expectations. In the cases of the dimethyl complexes **3a/4a**, the ³¹P nucleus in **4a** is better shielded than in **3a** (in most Pt(II) and Pd(II) phosphane complexes the reverse situation is typically observed [15]). In the di(pentafluorophenyl) complexes **3h/4h**, the δ³¹P values are very similar, although in this case the ³¹P nuclear shielding in **3h** is slightly increased relative to **4h**. The largest value for the coupling constant ¹J(¹⁹⁵Pt, ³¹P) is measured in **3h**, in agreement with the polarizing ability of the electronegative C₆F₅ group. It is remarkable that the magnitude of ¹J(¹⁹⁵Pt, ³¹P) = 2223 Hz in **3e** (R = CH₂Ph) is significantly larger than for the complexes with phenyl or alkyl substituents.

2.2.3. Signs of coupling constants

In the platinum(II) complexes, the presence of ¹H, ¹³C, ³¹P and ¹⁹⁵Pt nuclei gives rise to numerous spin–spin coupling interactions, of which the signs are known only in few cases. Thus, the sign of ¹J(¹⁹⁵Pt, ³¹P) is positive [16], and most likely, the sign of ²J(³¹P, ¹³C_{*trans*}) is also positive. In all other cases, experimental evidence of the coupling signs is desirable in order to make use of the numerical values. Relative signs of coupling constants can be readily obtained by appropriate one-dimensional (1D) heteronuclear double resonance ex-

Table 1
 ^{31}P , ^{195}Pt and ^{13}C NMR data ^{a,b} of **3a–g**, **3i** and **4a**

No.	$\delta^{31}\text{P}$	$\delta^{195}\text{Pt}$	$\delta^{13}\text{C}(\text{Pt}-\text{R})$	$\delta^{13}\text{C}(\text{C}^1)$	$\delta^{13}\text{C}(\text{C}^{2,7})$	$\delta^{13}\text{C}(\text{C}^{3,6})$	$\delta^{13}\text{C}(\text{C}^{4,5})$
3a	99.7 (s) {2000}	291.5 (d) {2001}	$\text{CH}_3^{\text{cis-Me}}$: -2.9 (d) [3.8] {784.0} $\text{CH}_3^{\text{trans-Me}}$: 15.7 (d) [116.6] {635.4}	34.1 (d) [21.8] {20.2}	117.6 (br)	127.1 (d) [9.8]	117.1 (br)
4a ^c	72.9 (s)	–	$\text{CH}_3^{\text{cis-Me}}$: -2.7 (d) [9.0] $\text{CH}_3^{\text{trans-Me}}$: 11.8 (d) [121.4]	35.7 (d) [12.6]	118.3 (br)	127.9 (d) [9.5]	122.5 (br)
3b ^d	95.6 (s) {1820}	198.4 (d) {1818}	$\text{CH}_2^{\text{cis-Et}}$: 10.7 (d) [2.7] {864.5} $\text{CH}_2^{\text{trans-Et}}$: 27.9 (d) [114.6] {707.7}	34.7 (d) [19.8] {19.5}	119.3 (s)	127.6 (d) [9.9]	116.6 (br)
3c ^e	96.1 (s) {1829}	237.3 (d) {1829}	$\text{CH}_2^{\text{cis-Pr}}$: 20.9 (d) [2.8] {858.7} $\text{CH}_2^{\text{trans-Pr}}$: 38.7 (d) [112.6] {705.4}	34.8 (d) [19.8] {19.5}	119.2 (br)	127.6 (d) [9.9]	99.3 (s)
3d ^f	95.8 (s) {1833}	229.8 (d) {1833}	$\text{CH}_2^{\text{cis-Bu}}$: 18.4 (s) {862.5} $\text{CH}_2^{\text{trans-Bu}}$: 35.8 (d) [112.9]	34.7 (d) [19.7] {19.0}	119.1 (br)	127.4 (d) [9.8]	99.1 (s)
3e ^g	92.6 (s) {2223}	214.3 (d) {2223}	$\text{CH}_2^{\text{cis-Bz}}$: 22.7 (d) [3.2] {800.3} $\text{CH}_2^{\text{trans-Bz}}$: 39.3 (d) [101.3] {605.2}	34.3 (d) [21.3] {18.8}	120.0 (s)	127.7 (d) [10.0]	116.6 (br)
3f ^h	89.8 (s) {1975}	263.8 (d) {1975}	$\text{C}_{\text{ipso}}^{\text{cis-Ph}}$: 149.1 (d) [7.6] {1114.3} $\text{C}_{\text{ipso}}^{\text{trans-Ph}}$: 168.7 (d) [126.7] {842.7}	34.6 (d) [23.4] {16.4}	120.2 (s)	127.2 (d) [11.3]	119.7 (br)
3g ^{i,j}	89.8 (s) {2025}	281.9 (ddd) {2025} <31.7> <32.1>	$\text{C}_{\text{ipso}}^{\text{cis}}$: 142.3 (d) [10.3] $\text{C}_{\text{ipso}}^{\text{trans}}$: 162.5 (d) [118.5]	34.5 (d) [25.3] {16.1}	120.5 (s)	127.7 (d) [9.6]	119.8 (br)
3i ^k	99.4 (s) {2139}	235.8 (d) {2138}	$\text{C}_1^{\text{cis-Fc}}$: 84.1 (d) [6.7] {1284.1} $\text{C}_1^{\text{trans-Fc}}$: 110.8 (d) [141.1] {975.6}	34.6 (d) [22.4]	117.7 (br)	130.6 (br)	127.3 (br)

^a Measurements in CDCl_3 (25 °C); *cis* and *trans* refer to the position of R relative to phosphorus.

^b Coupling constants {} $^n J(^{195}\text{Pt}, \text{X})$, [] $^n J(^{31}\text{P}, ^{13}\text{C})$ in Hz.

^c Measurement in CD_2Cl_2 (25 °C).

^d $\delta^{13}\text{C}(\text{R})$: 14.9 (d, [5.4] {23.7}), $\text{CH}_3^{\text{trans-Et}}$, 17.0 (s, {35.5}), $\text{CH}_3^{\text{cis-Et}}$.

^e $\delta^{13}\text{C}(\text{R})$: 24.1 (d, [3.5] {7.6}), $\text{CH}_2^{\text{trans-Pr}}$, 24.6 (s, {25.7}), $\text{CH}_2^{\text{cis-Pr}}$, 19.3 (s, {147.5}), $\text{CH}_3^{\text{cis-Pr}}$, 19.9 (d, [10.0] {92.6}), $\text{CH}_3^{\text{trans-Pr}}$.

^f $\delta^{13}\text{C}(\text{R})$: 28.0 (s, {137.4}), $(\text{CH}_2)_2^{\text{cis/trans-Bu}}$, 28.4 (d, [9.9] {92.9}), $(\text{CH}_2)_2^{\text{cis/trans-Bu}}$, 34.6 (s, $(\text{CH}_2)_2^{\text{cis/trans-Bu}}$), 33.4 (d, [4.7]), $(\text{CH}_2)_2^{\text{cis/trans-nBu}}$, 14.0/14.5 (s/s, $\text{CH}_3^{\text{cis/trans-Bu}}$).

^g $\delta^{13}\text{C}(\text{R})$: 148.8 (d, [2.6] {56.0}), $\text{C}_{\text{ipso-cis}}$, 150.1 (d, [5.5] {48.9}), $\text{C}_{\text{ipso-trans}}$, 127.3 (s, {14.3}), $\text{C}_{\text{meta-cis}}$, 128.3 (d, [3.6] {26.2}), $\text{C}_{\text{meta-trans}}$, 127.4 (d, [1.8] {n.o.}), $\text{C}_{\text{ortho-trans}}$, 129.5 (s, {49.1}), $\text{C}_{\text{ortho-cis}}$, 122.1 (d, [2.3] {15.1}), $\text{C}_{\text{para-trans}}$, 122.9 (s, {20.2}), $\text{C}_{\text{para-cis}}$.

^h $\delta^{13}\text{C}(\text{R})$: 127.3 (d, [1.7] {89.4}), $\text{C}_{\text{meta-cis}}$, 127.7 (d, [7.1] {61.1}), $\text{C}_{\text{meta-trans}}$, 135.3 (s, {32.0}), $\text{C}_{\text{ortho-cis}}$, 135.4 (d, [2.6] {29.0}), $\text{C}_{\text{ortho-trans}}$, 121.9 (d, [1.6] {14.1}), $\text{C}_{\text{para-trans}}$, 122.5 (d, [1.1] {10.1}), $\text{C}_{\text{para-cis}}$.

ⁱ $\langle \rangle$: $^5 J(^{195}\text{Pt}, ^{19}\text{F})$ or $^n J(^{19}\text{F}, ^{13}\text{C})$ in Hz.

^j $\delta^{13}\text{C}(\text{R})$: 114.1 (d, 1<8.6> {97.2}), $\text{C}_{\text{meta-cis}}$, 114.4 (dd, [8.9] 17.8 {n.o.}), $\text{C}_{\text{meta-trans}}$, 135.3 (dd, [2.5] <5.3> {n.o.}), $\text{C}_{\text{ortho-trans}}$, 135.4 (d, 5.5 {40.5}), $\text{C}_{\text{ortho-cis}}$.

^k $\delta^{13}\text{C}(\text{R})$: 75.1/ 77.2 (d/d, [5.6] {57.0}/[5.0] {79.1}), $\text{C}^{2,5(\text{Fc})-\text{trans/cis}}$, 67.8/ 69.2 (s/s, $\text{C}^{3,4(\text{Fc})-\text{cis/trans}}$), 67.4/ 68.2 (s/s, $\text{C}_{\text{cis/trans-Cp}(\text{Fc})}$).

Table 2
 ^{31}P , ^1H and ^{13}C NMR data ^a of **3h** and **4h**

No.	3h	4h
(1) $\delta^{31}\text{P}^b$	97.8 (s) {2707}	101.0 (m)
(2) $\delta^1\text{H}^c$		d
Free rings:		
H ¹	2.14 (dt, 2H) (6.7) [9.0]	1.97 (dt, 2H) (6.6) [8.4]
H ^{2,7}	4.83 (m, 2H) [7.0] 5.09 (m, 2H) [6.4]	4.73 (m, 2H) [7.3] 5.07 (m, 2H) [7.1]
H ^{3,6}	6.25 (m, 4H)	6.23 (m, 4H)
H ^{4,5}	6.63 (m, 4H)	6.62 (m, 4H)
Coordinated ring:		
H ^{1'}	4.80 (m, 1H)	4.45 (dt, 1H) (8.6) [13.1]
H ^{2',7'}	5.83 (m, 2H) [9.1]	5.81 (m, 2H) [8.6]
H ^{3',6'}	6.56 (m, 2H)	6.72/6.62 (m/m, 4H)
H ^{4',5'}	6.05 (m, 2H) {44.3}	
(3) $\delta^{13}\text{C}^e$		f
Free rings:		
C ¹	35.0 (d) [32.7] {45.2}	35.4 (d) [24.9]
C ^{2,7}	113.7 (s) {17.4}	114.3 (s)
	114.3 (s) {16.7}	115.2 (s)
C ^{3,6}	127.0 (d) [11.0]	126.9 (d) [11.3]
	127.4 (d) [10.5]	127.3 (d) [9.8]
C ^{4,5}	131.0 (s)	130.9 (s)
	131.2 (s)	131.1 (s)
Coordinated ring:		
C ^{1'}	36.3 (d) [22.1] {17.2}	38.5 (d) [12.2]
C ^{2',7'}	129.9 (s) {49.6}	130.5 (s)
C ^{3',6'}	130.4 (d) [10.3]	130.3 (d) [9.7]
C ^{4',5'}	93.8 (s) {51.7}	107.5 (s)

^a Measurements in CD_2Cl_2 at 25 °C; ^{13}C NMR data of C_6F_5 groups not assigned.

^b Coupling Constant { } $^1J(^{195}\text{Pt}, ^{31}\text{P})$ in Hz.

^c Coupling Constants { } $^nJ(^{195}\text{Pt}, ^1\text{H})$, [] $^2J(^{31}\text{P}, ^1\text{H})$, () $^nJ(^1\text{H}, ^1\text{H})$ in Hz.

^d Measurement at -20 °C.

^e Coupling constants { } $^nJ(^{195}\text{Pt}, ^{13}\text{C})$, [] $^1J(^{31}\text{P}, ^{13}\text{C})$ in Hz.

^f Measurement at 0 °C.

periments [17] or by 2D heteronuclear shift correlations (HETCOR) [18], in which one nucleus (neither irradiated nor observed) is the passive spin, and the other two (irradiated or observed) are the active spins. The coupling signs to be compared refer to couplings between the active and the passive spins.

The results of typical 1D experiments are shown in Fig. 3 for $[\text{P}]\text{PtMe}_2$ **3a**, where the signs of $^3J(^{31}\text{P}, \text{Pt}, \text{C}^1, \text{H})$ and $^1J(^{195}\text{Pt}, ^{31}\text{P})$ are compared via selective heteronuclear $^1\text{H}\{^{195}\text{Pt}\}$ double resonance experiments. Figs. 4 and 5 show typical examples of the application of 2D HETCOR experiments. In the case of **3a**, a negative tilt of the ^{195}Pt satellite cross peaks is observed for both PtMe groups in $^{31}\text{P}/^1\text{H}$ shift correlations. As expected [19], all signs $^1J(^{195}\text{Pt}, ^{13}\text{C}_{\text{Me}, \text{Et}})$ are positive, and all signs $^2J(^{195}\text{Pt}, ^1\text{H}_{\text{Me}, \text{Et}})$ are negative. The $^{195}\text{Pt}/^1\text{H}$ shift correlation shown in Fig. 5 for CH_2 of the ethyl group in *cis*-position with respect to phosphorus, proves that

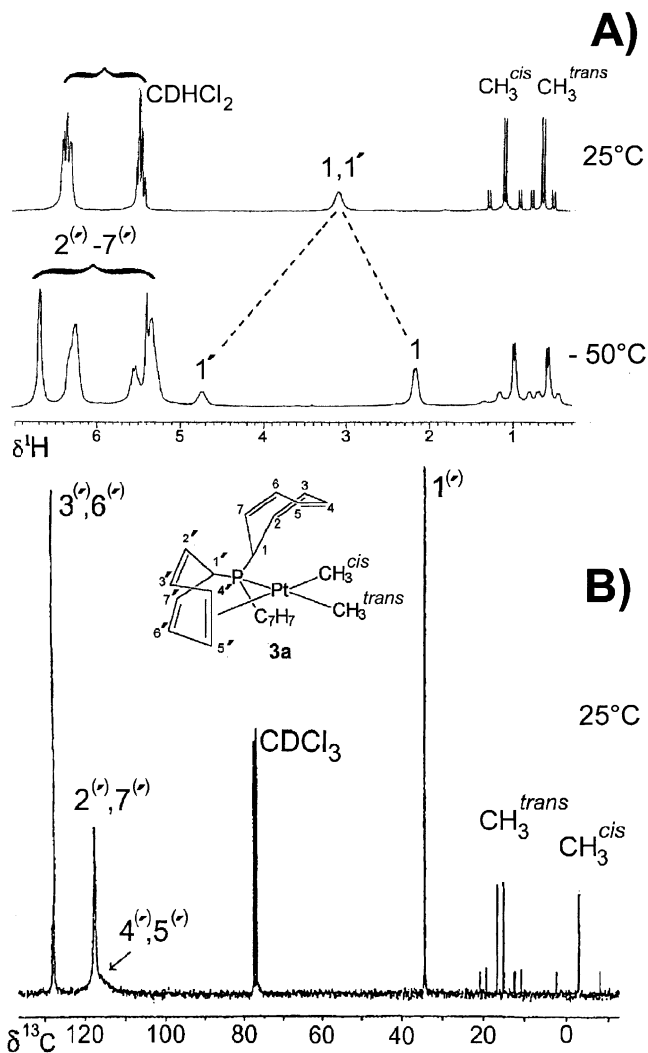


Fig. 1. (A) 250 MHz ^1H NMR spectra of $[\text{P}]\text{PtMe}_2$ (**3a**) (in CD_2Cl_2) at room temperature and at -50 °C. Note that the PtMe groups show nicely resolved different signals in spite of the dynamic process involving the intramolecular exchange of the C_7H_7 rings. (B) 62.9 MHz $^{13}\text{C}\{^1\text{H}\}$ NMR spectrum of $[\text{P}]\text{PtMe}_2$ (**3a**) (in CDCl_3) at room temperature. The $^{13}\text{C}(\text{PtMe})$ signals are different, whereas the $^{13}\text{C}(\text{C}_7\text{H}_7)$ signals are broad or sharp singlets owing to exchange of the C_7H_7 rings.

$^1J(^{195}\text{Pt}, ^{31}\text{P})$ (>0) and $^3J(^{31}\text{P}, \text{Pt}, \text{C}, ^1\text{H}_{\text{cis}})$ are alike. From $^1\text{H}/^1\text{H}$ COSY experiments carried out for **3b**, by observing the ^{195}Pt satellite cross peaks, it follows that the sign of $^3J(^{195}\text{Pt}, ^1\text{H}_{\text{Et}})$ is positive. For the coordinated $\eta^2\text{-C}=\text{C}$ bond, the sign of $^1J(^{195}\text{Pt}, ^{13}\text{C})$ is also positive, and that of $^2J(^{195}\text{Pt}, ^1\text{H})$ is negative. The magnitude of the coupling constants $|^3J(^{31}\text{P}, \text{Pt}, \text{C}, ^1\text{H})|$ is almost identical for both PtMe groups in **3a** (7.6 and 6.8 Hz). However, their signs are opposite (Fig. 3), a negative sign is found for $^3J(^{31}\text{P}, \text{Pt}, \text{C}, ^1\text{H}_{\text{trans}})$ and a positive sign for $^3J(^{31}\text{P}, \text{Pt}, \text{C}, ^1\text{H}_{\text{cis}})$. The data $^2J(^{195}\text{Pt}, ^{13}\text{C}^{1,1'})$ are also of interest since the absolute sign of $^2J(^{195}\text{Pt}, ^{13}\text{C}^1)$ (>0) has been determined in a non-fluxional cationic complex $\{[\text{P}]\text{Pt}(\text{Cp})\}^+$ [7]. In **3h**

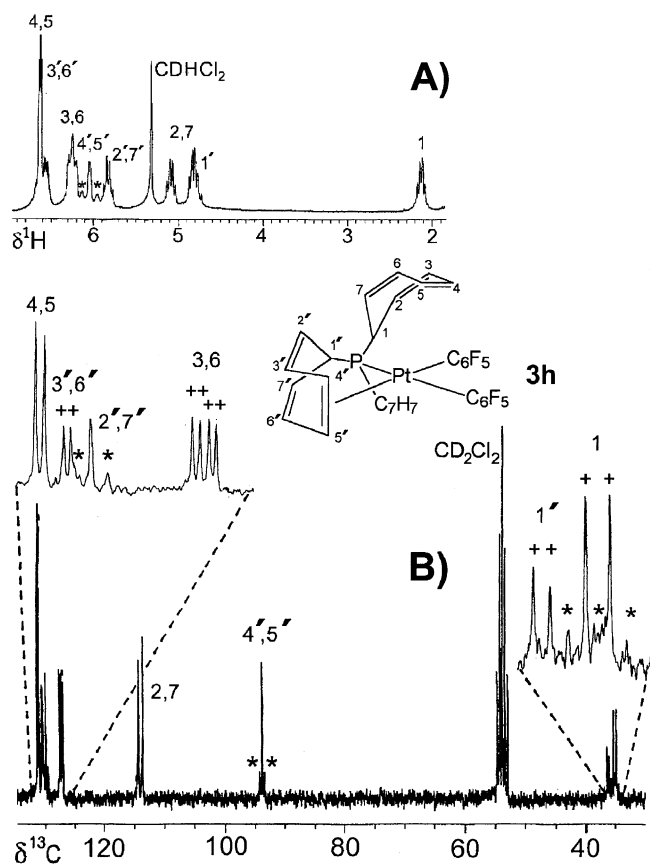


Fig. 2. (A) 250 MHz ^1H NMR spectrum of $[\text{P}]\text{Pt}(\text{C}_6\text{F}_5)_2$ (**3h**) (in CD_2Cl_2) at room temperature. The dynamic process of exchanging C_7H_7 rings is slow on the NMR time scale and most signals for coordinated and non-coordinated C_7H_7 rings are clearly resolved (satellites due to $J(^{195}\text{Pt}, ^1\text{H})$ are marked by asterisks). (B) 62.9 MHz $^{13}\text{C}\{^1\text{H}\}$ NMR spectrum of $[\text{P}]\text{Pt}(\text{C}_6\text{F}_5)_2$ (**3h**) (in CD_2Cl_2) at room temperature. The signals for coordinate and non-coordinate C_7H_7 rings are resolved (doublets due to $J(^{31}\text{P}, ^{13}\text{C})$ are marked by + and satellites due to $J(^{195}\text{Pt}, ^{13}\text{C})$ are marked by *).

(see Fig. 2), the magnitude of $|^2J(^{195}\text{Pt}, ^{13}\text{C}^{1'})|$ (17.2 Hz) and $|^2J(^{195}\text{Pt}, ^{13}\text{C}^1)|$ (45.2 Hz) can be measured, whereas in the other complexes studied here only the averaged magnitude $|^2J(^{195}\text{Pt}, ^{13}\text{C}^{1,1'})|$ was accessible. These mean values (≈ 20 Hz) indicate that the signs of the coupling constants $^2J(^{195}\text{Pt}, ^{13}\text{C}^{1'})$ and $^2J(^{195}\text{Pt}, ^{13}\text{C}^1)$ are most likely opposite. A similar trend is also evident for the values $|^2J(^{195}\text{Pt}, ^{13}\text{C}^{1,1'})|$ in the halides $[\text{P}]\text{PtX}_2$ [6].

2.3. X-ray structural analysis of $[\text{P}]\text{Pt}(\text{C}_6\text{H}_4\text{-4-F})_2$ (**3g**)

The molecular structure of **3g** is shown in Fig. 6, together with selected bond lengths and angles. The phosphane [P] acts as a bidentate chelating ligand which occupies two adjacent positions of the square planar arrangement around the platinum atom (mean deviation from plane: 5 pm). The remaining two positions are

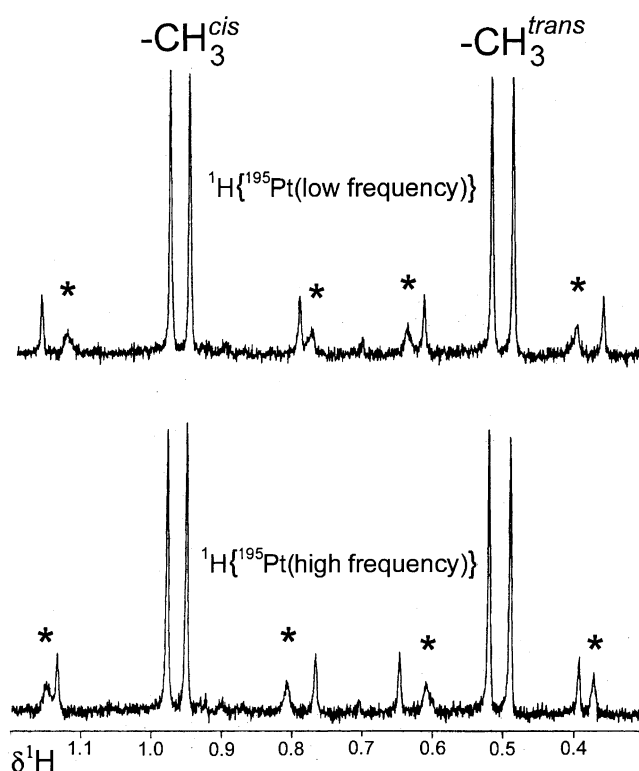


Fig. 3. Heteronuclear $^1\text{H}\{^{195}\text{Pt}\}$ spin tickling experiment, showing the $^1\text{H}(\text{PtMe})$ resonances of **3a** upon low power selective irradiation of the ^{195}Pt transitions (transitions influenced by irradiation with the ^{195}Pt frequency are indicated by asterisks). This compares the signs of $^1J(^{195}\text{Pt}, ^31\text{P})$ (> 0) with those of $^3J(^{31}\text{P}, \text{Pt}, \text{C}, ^1\text{H}_{\text{Me-cis/trans}})$. The sign of the latter coupling constant involving of the $^1\text{H}(\text{PtMe}_{\text{cis}})$ nuclei at higher frequency is positive whereas the other one for $^1\text{H}(\text{PtMe}_{\text{trans}})$ at lower frequency is negative (note that the absolute magnitudes of these coupling constants $^3J(^{31}\text{P}, \text{Pt}, \text{C}, ^1\text{H})$ are almost identical).

taken by the $\text{C}_6\text{H}_4\text{-4-F}$ groups, of which the benzene ring planes are oriented almost perpendicular (83.9°) to each other. This particular geometry, present only in the solid state, appears to be typical of diaryl-Pt(II) complexes [20,21]. The plane of the $\text{C}_6\text{H}_4\text{-4-F}$ group in *trans*-position with respect to the η^2 -coordinated $\text{C}=\text{C}$ bond is twisted by only 8.4° against the PtCC plane. For clarity, the coordination geometry of platinum and the positions of the $\text{C}_6\text{H}_4\text{-4-F}$ ligands are shown in detail in Fig. 7. Since the arrangement of the $\text{C}_6\text{H}_4\text{-4-F}$ groups is not enforced by steric constraints, (dp) π interactions between platinum and the aryl groups are likely, in agreement with the changes in the $^{13}\text{C}(4)$ nuclear magnetic shielding in solution when compared with C_6H_6 and $\text{C}_6\text{H}_5\text{-F}$. Although aryl rotation about the Pt–C(aryl) axis is fast in solution, the $^{13}\text{C}(4)$ chemical shifts indicate preference of a preferred conformation which, most likely, corresponds to that found for the solid state. As in other $[\text{P}]\text{Pt}(\text{L})(\text{L}')$ complexes (cf. [6,9–11]), where the Pt–L bond *trans* to phosphorus is longer than the Pt–L' bond *trans* to the η^2 -coordinated $\text{C}=\text{C}$

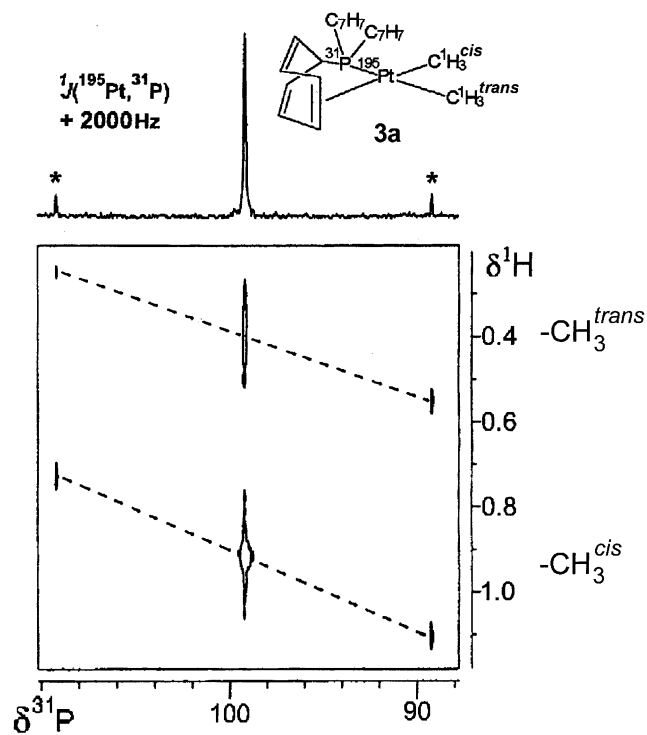


Fig. 4. Contour plot of the 2D 101.25 MHz $^{31}\text{P}/^1\text{H}$ HETCOR experiment based on the coupling constants $^3J(^{31}\text{P}, \text{Pt}, \text{C}, ^1\text{H}_{\text{Me}}) \approx 7$ Hz. The negative tilt of the cross peaks for the ^{195}Pt satellites proves that for both methyl groups the signs of the coupling constants $^2J(^{195}\text{Pt}, ^1\text{H})$ and $^1J(^{195}\text{Pt}, ^{31}\text{P})$ are opposite. Since the latter sign is known to be positive, it follows that $^2J(^{195}\text{Pt}, ^1\text{H}) < 0$.

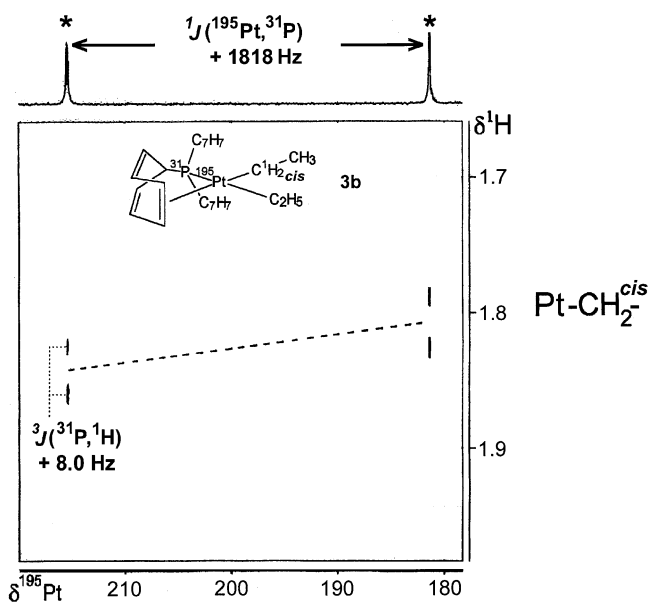


Fig. 5. Contour plot of the 2D 53.5 MHz $^{195}\text{Pt}/^1\text{H}$ HETCOR experiment based on the coupling constant $^2J(^{195}\text{Pt}, ^1\text{H}_{\text{Et}}) = 101$ Hz, using a BIRD pulse sequence for homonuclear $^1\text{H}, ^1\text{H}$ decoupling. The part of the $^1\text{H}(\text{CH}_2^{\text{cis}})$ resonances is shown, with a splitting due to $^3J(^{31}\text{P}, \text{Pt}, \text{C}, ^1\text{H})$, and a positive tilt of the cross peaks which indicates that the signs of the coupling constants $^1J(^{195}\text{Pt}, ^{31}\text{P})$ and $^3J(^{31}\text{P}, \text{Pt}, \text{C}, ^1\text{H})$ are alike.

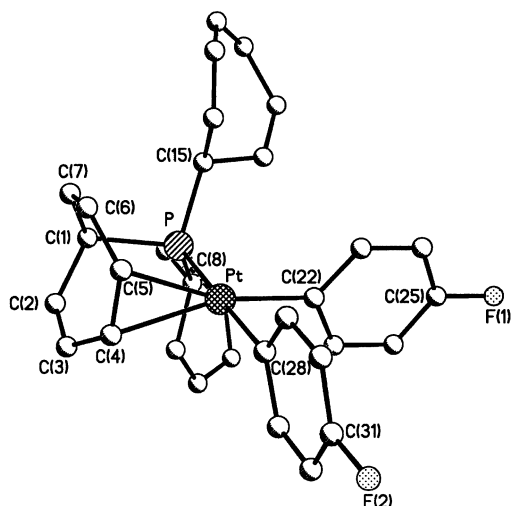


Fig. 6. Molecular structure of $[\text{P}]\text{Pt}(\text{C}_6\text{H}_4-4\text{-F})_2$ (**3g**) (hydrogen atoms are omitted for clarity). Selected bond lengths [pm] and angles [degrees]: Pt–P 229.37(17), Pt–C(22) 203.5(6), Pt–C(28) 207.7(6), Pt–C(4) 229.7(7), Pt–C(5) 231.3(6), C(1)–C(2) 150.5(10), C(1)–C(7) 151.4(10), C(2)–C(3) 133.5(10), C(3)–C(4) 146.9(10), C(4)–C(5) 138.6(10), C(5)–C(6) 144.8(11), C(6)–C(7) 131.6(11), C(11)–C(12) 132.0(14), C(18)–C(19) 134.9(12), P–C(1) 187.5(7), P–C(8) 185.8(7), P–C(15) 184.8(7), C(25)–F(1) 137.1(8), C(31)–F(2) 138.5(9); C(22)–Pt–C(28) 85.9(2), C(22)–Pt–P 92.47(18), C(28)–Pt–P 178.22(19), C(22)–Pt–C(4) 162.9(3), C(22)–Pt–C(5) 161.5(3), C(28)–Pt–C(4) 90.0(3), C(28)–Pt–C(5) 91.1(3), P–Pt–C(4) 91.78(18), P–Pt–C(5) 90.21(19).

bond, the respective Pt–C(28) and Pt–C(22) bond lengths in **3g** differ in a similar way (207.7(6) and 203.5(6) pm). The Pt–C(4) and Pt–C(5) bonds (η^2 -coordinated C=C bond) are almost identical (229.7(7) and 231.3(6) pm), and they are longer than the bonds

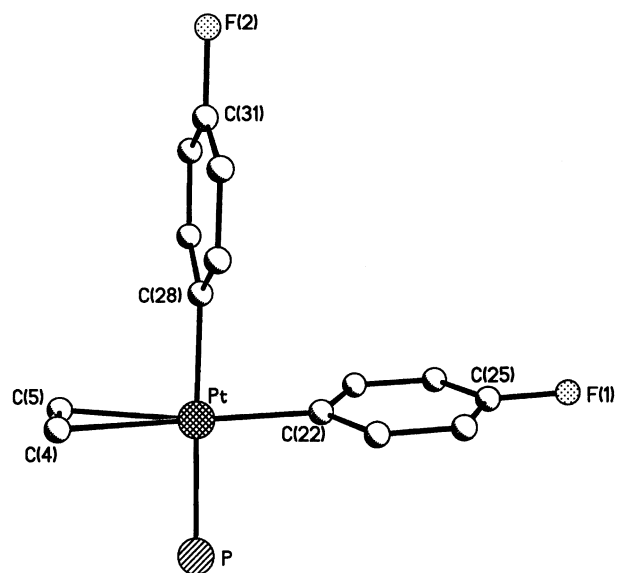


Fig. 7. The geometry around platinum in $[\text{P}]\text{Pt}(\text{C}_6\text{H}_4-4\text{-F})_2$ (**3g**) as determined by X-ray analysis. Note the orientation of the $\text{C}_6\text{H}_4-4\text{-F}$ groups, the dihedral angle between the two 4-fluorophenyl ring planes is 83.9° .

Pt–C(28) and Pt–C(22). Both non-coordinated C₇H₇ rings are linked to the phosphorus atom by equatorial P–C bonds. This suggests that the bonding situation of the ligand [P] has to change considerably in going from the solid to the solution state (in contrast to one example of a Rh(I) complex noted in the literature [13]). The dynamic process in solution requires spatial proximity of at least a second C₇H₇ ring to the platinum atom, and also an axial P–C bond of this particular ring in order to substitute the coordinated ring. These features are not observed in the solid-state molecular structure of **3g**.

3. Conclusions

The synthesis of stable complexes of Pt(II) and Pd(II) containing the bidentate ligand [P] and two organyl groups R is straightforward. These complexes are fluxional, the Pd(II) more than the Pt(II) species, with respect to η^2 -C=C coordination of the C₇H₇ rings in [P]. In this dynamic process, the stereochemistry of the groups R remains fixed, pointing towards an associative mechanism involving a transition state with five-coordinate Pt. There is a wealth of coupling constants available in the complexes studied. Although most of the coupling signs are found as expected, in several cases opposite signs were determined or had to be invoked in order to make use of the numerical values.

4. Experimental section

4.1. General and starting materials

All compounds were synthesized and handled in an atmosphere of dry argon, and carefully dried solvents were used throughout. Starting materials were prepared according to literature procedures, e.g. P(C₇H₇)₃ [5], [P]MCl₂ (**1**) and **2** [6], and FcLi [22], or were used as commercial products without further purification, e.g. Mg, RBr (R = Et, Pr, Bu, CH₂Ph, Ph, C₆F₅), 4-F-C₆H₄MgBr (1 M in THF), MeLi (1.6 M in Et₂O) and ⁿBuLi (1.6 M in hexane).

4.1.1. NMR spectroscopy

Bruker ARX 250 or DRX 500 (¹H, ¹³C, ³¹P, ¹⁹⁵Pt NMR); chemical shifts are given with respect to Me₄Si [$\delta^1\text{H}$ (CD(H)Cl₂) = 5.33; $\delta^{13}\text{C}$ (CD₂Cl₂) = 50.3; external aqueous H₃PO₄ (85%) with $\delta^{31}\text{P} = 0$ for $\Xi(^{31}\text{P}) = 40.480747$ MHz, and $\delta^{195}\text{Pt} = 0$ for $\Xi(^{195}\text{Pt}) = 21.400000$ MHz. Heteronuclear ¹H{X} experiments (X = ³¹P, ¹⁹⁵Pt) were carried out by using the known (from X NMR spectra) frequencies for the X transitions, and by adjusting the power level (usually values > 40 dB) in order to induce the selective effects. The 2D HETCOR experiments, based on $J(\text{X}, ^1\text{H})$ (X = ¹³C, ³¹P,

¹⁹⁵Pt), were optimised in 1D INEPT experiments. Because of fast ¹⁹⁵Pt nuclear spin relaxation (chemical shift anisotropy relaxation mechanism, dependent on B₀²), the ¹⁹⁵Pt/¹H shift correlations gave a better performance at lower field strengths B₀.

EI MS: Finnigan MAT 8500 (Ionisation energy 70 eV).

4.2. Synthesis of [P]PtMe₂ (**3a**)

A suspension of [P]PtCl₂ (**1**) (171 mg, 0.30 mmol) in a toluene/Et₂O mixture (20 ml/5 ml) was reacted with 0.5 ml of a 1.6 M MeLi/Et₂O solution (0.8 mmol) at –78 °C. The reaction mixture was allowed to warm up to room temperature and stirred for further 30 min, before it was cooled again to –78 °C and an excess of water was added. The mixture was again brought to ambient temperature, the organic layer was separated and the solvent was removed in vacuo. The residue was washed with hexane (50 ml), recrystallized from CH₂Cl₂/hexane and dried in a high vacuum.

4.2.1. [P]PtMe₂ (**3a**)

Bright-yellow powder, dec. 159 °C, yield 125 mg (79%). ¹H NMR (CDCl₃, 25 °C): $\delta = 0.54$ (d, 3H, H^{trans}-Me; $^2J(^{31}\text{P}, ^1\text{H}) = 7.6$ Hz, $^3J(^{195}\text{Pt}, ^1\text{H}) = 63.3$ Hz), 1.02 (d, 3H, H^{cis}-Me; $^2J(^{31}\text{P}, ^1\text{H}) = 6.8$ Hz, $^3J(^{195}\text{Pt}, ^1\text{H}) = 99.0$ Hz), 3.91 (br, 3H, H¹), 5.28 (m, 6H, H^{2,7}), 6.12 (br, 6H, H^{4,5}), 6.20 (m, 6H, H^{3,6}). C₂₃H₂₇PPt, EI MS: *m/e* (%) = 514 (73) [P(C₇H₇)₃PtMe⁺], 423(4) [P(C₇H₇)₂PtMe⁺], 332(5) [P(C₇H₇)PtMe⁺], 91(100) [C₇H₇⁺].

4.3. Synthesis of [P]PdMe₂ (**4a**)

An ethereal solution of 1.6 M MeLi (0.8 ml, 1.3 mmol) was added to a suspension of [P]PdCl₂ (**2**) (120 mg, 0.25 mmol) in a toluene/Et₂O mixture (20 ml/5 ml) at –78 °C. The reaction mixture was immediately brought to room temperature and then stirred for 1.5 h. Hydrolysis with water (30 ml) at –50 °C gave a two-phase mixture. After filtration the organic layer was separated and the solvents removed in vacuo. The remaining residue was dissolved in CH₂Cl₂ (2 ml) and pentane was added (20 ml). The bright-brown product **4a** which precipitated at –80 °C overnight was dried under high vacuum.

4.3.1. [P]PdMe₂ (**4a**)

Bright-brown powder, dec. 127 °C, yield 67 mg (61%). ¹H NMR (CDCl₃, 25 °C): $\delta = 0.16$ (d, 3H, H^{cis}-Me; $^2J(^{31}\text{P}, ^1\text{H}) = 7.3$ Hz), 0.49 (d, 3H, H^{trans}-Me; $^2J(^{31}\text{P}, ^1\text{H}) = 8.0$ Hz), 2.74 (dt, 3H, H¹; $^2J(^{31}\text{P}, ^1\text{H}) = 7.4$ Hz, $^3J(^1\text{H}, ^1\text{H}) = 7.4$ Hz), 5.27 (m, 6H, H^{2,7}), 6.26 (m, 6H, H^{4,5}), 6.48 (m, 6H, H^{3,6}). C₂₃H₂₇PPd, EI MS:

m/e (%) = 425(1) [P(C₇H₇)₃PdMe⁺], 410 (<1) [P(C₇H₇)₃Pd⁺], 91 (100) [C₇H₇⁺].

4.4. General procedure for the synthesis of [P]PtR₂ (R = Et **3b**, Pr **3c**, Bu **3d**, Bz **3e**, Ph **3f**)

At 0 °C solid [P]PtCl₂ (**1**) (285 mg, 0.5 mmol) was added to a RMgBr solution, which had been prepared from Mg (50 mg, 2.1 mmol) and RBr (R = Et, Pr, Bu, Bz) (2.00 mmol) in Et₂O (20 ml). The reaction mixture was stirred for 4 h at 0 °C, then a cold saturated, aqueous NH₄Cl solution was added. The organic layer was separated and the solvent was removed in vacuo. The residue was recrystallized from CH₂Cl₂/hexane and dried in a high vacuum.

4.4.1. [P]PtEt₂ (**3b**)

Bright-yellow powder, dec. 165 °C, yield 242 mg (87%). ¹H NMR (CDCl₃, 25 °C): δ = 1.07 (t, 3H, H^{cis-Et}; ³J(¹⁹⁵Pt, ¹H) = 100.7 Hz, ³J(¹H, ¹H) = 7.8 Hz), 1.13 (m, 2H, H^{trans-Et}; ³J(³¹P, ¹H) = 8.5 Hz, ³J(¹H, ¹H) = 6.5 Hz), 1.26 (dt, 3H, H^{trans-Et}; ³J(¹⁹⁵Pt, ¹H) = 64.7 Hz, ⁴J(³¹P, ¹H) = 8.2 Hz, ³J(¹H, ¹H) = 6.1 Hz), 1.83 (m, 2H, H^{cis-Et}; ²J(¹⁹⁵Pt, ¹H) = 95.0 Hz, ³J(³¹P, ¹H) = 8.0 Hz, ³J(¹H, ¹H) = 7.4 Hz), 2.89 (br, 3H, H¹), 5.32 (m, 6H, H^{2,7}), 6.16 (m, 6H, H^{3,6}), 6.20 (br, 6H, H^{4,5}). C₂₅H₃₁PPt, EI MS: *m/e* (%) = 528(3) [P(C₇H₇)₃PtEt⁺]; 499(20) [P(C₇H₇)₃Pt⁺]; 408(5) [P(C₇H₇)₂Pt⁺], 91(100) [C₇H₇⁺].

4.4.2. [P]PtPr₂ (**3c**)

Yellow powder, dec. 111 °C, yield 211 mg (72%). ¹H NMR (CDCl₃, 25 °C): δ = 0.80 (t, 3H, H^{cis/trans-Pr}; ³J(¹H, ¹H) = 7.0 Hz), 1.04 (t, 3H, H^{cis/trans-Pr}; ³J(¹H, ¹H) = 7.2 Hz), 1.10–1.97 (m/m/m/m, 8H, H^{cis/trans-Pr}), 2.90 (br, 3H, H¹), 5.31 (m, 6H, H^{2,7}), 6.16 (m, 6H, H^{3,6}), 6.20 (br, 6H, H^{4,5}). C₂₇H₃₅PPt, EI MS: *m/e* (%) = 542(2) [P(C₇H₇)₃PtPr⁺], 499(9) [P(C₇H₇)₃Pt⁺], 304(8) [P(C₇H₇)₃⁺], 91(100) [C₇H₇⁺].

4.4.3. [P]PtBu₂ (**3d**)

Yellow powder, dec. 124 °C, yield 233 mg (76%). ¹H NMR (CDCl₃, 25 °C): δ = 0.74 (t, 3H, H^{cis/trans-Bu}; ³J(¹H, ¹H) = 7.2 Hz), 0.92 (t, 3H, H^{cis/trans-Bu}; ³J(¹H, ¹H) = 7.3 Hz), 1.08–1.82 (m/m/m/m, 12H, H^{cis/trans-Bu}), 2.90 (br, 3H, H¹), 5.31 (m, 6H, H^{2,7}), 6.15 (m, 6H, H^{3,6}), 6.20 (br, 6H, H^{4,5}).

4.4.4. [P]PtBz₂ (**3e**)

Yellow powder, dec. 133 °C, yield 259 mg (76%). ¹H NMR (CDCl₃, 25 °C): δ = 2.71 (d, 2H, H^{trans-Bz}; ²J(³¹P, ¹H) = 11.2 Hz, ³J(¹⁹⁵Pt, ¹H) = 91.0 Hz), 2.93 (br, 3H, H¹), 3.28 (d, 2H, H^{cis-Bz}; ²J(³¹P, ¹H) = 7.2 Hz, ³J(¹⁹⁵Pt, ¹H) = 122.6 Hz), 5.38 (m, 6H, H^{2,7}), 6.13 (br, 6H, H^{4,5}), 6.23 (m, 6H, H^{3,6}), 6.80–7.35 (m, 10H, H^{cis/trans-Bz}). C₃₅H₃₅PPt, EI MS: *m/e* (%) = 681(1)

[M⁺], 590(100) [P(C₇H₇)₃PtBz⁺], 499(8) [P(C₇H₇)₃Pt⁺], 408(7) [P(C₇H₇)₂Pt⁺], 304(2) [P(C₇H₇)₃⁺], 91(91) [C₇H₇⁺].

4.4.5. [P]PtPh₂ (**3f**)

Bright-yellow powder, dec. 127 °C, yield 265 mg (81%). ¹H NMR (CDCl₃, 25 °C): δ = 2.77 (br, 3H, H¹), 5.18 (m, 6H, H^{2,7}), 6.26 (m, 6H, H^{3,6}), 6.31 (br, 6H, H^{4,5}), 6.57–7.68 (m, 10H, H^{cis/trans-Ph}). C₃₃H₃₁PPt, EI MS: *m/e* (%) = 499(5) [P(C₇H₇)₃Pt⁺], 408(6) [P(C₇H₇)₂Pt⁺], 304(1) [P(C₇H₇)₃⁺], 154(100) [C₆H₅–C₆H₅⁺], 91(51) [C₇H₇⁺], 78(12) [C₆H₆⁺].

4.5. Synthesis of [P]Pt(C₆H₄–4-F)₂ (**3g**)

A 1.0 M BrMgC₆H₄–4-F solution (2.6 ml, 2.6 mmol) in THF was added to a suspension of [P]PtCl₂ **1** (285 mg, 0.50 mmol) in Et₂O (15 ml) at 0 °C. The reaction mixture was stirred at room temperature for 3.5 h. After hydrolysis with water (10 ml) at 0 °C, the organic layer was separated and brought to dryness in vacuo. The residue was recrystallized from CH₂Cl₂/pentane and dried in a high vacuum.

4.5.1. [P]Pt(*p*-C₆H₄F)₂ (**3g**)

Bright-yellow powder, dec. 161 °C, yield 245 mg (71%). ¹H NMR (CDCl₃, 25 °C): δ = 2.76 (br, 3H, H¹), 5.19 (m, 6H, H^{2,7}), 6.26 (m, 6H, H^{3,6}), 6.29 (br, 6H, H^{4,5}), 6.54/6.81 (m/m, 2H/2H, H^{meta-cis/trans}), 7.01/7.43 (m/m, 2H/2H, H^{ortho-cis/trans}). C₃₃H₂₉F₂PPt, EI MS: *m/e* (%) = 503(1) [P(C₇H₇)₂Pt(C₆H₄F)⁺], 499(7) [P(C₇H₇)₃Pt⁺], 408(6) [P(C₇H₇)₂Pt⁺], 190(26) [C₆H₄F–C₆H₄F⁺], 91(100) [C₇H₇⁺].

4.6. General procedure for the synthesis of [P]M(C₆F₅)₂ (M = Pt **3h**, M = Pd **4h**)

A C₆F₅Li solution (≈0.45 mmol) was freshly prepared from C₆F₅Br (60 μl, 121 mg, 0.49 mmol) and a 1.6 M BuLi/Et₂O solution (0.3 ml, 0.49 mmol) in Et₂O (5 ml). Then Et₂O (15 ml) was added and the solution cooled to –78 °C, before [P]MCl₂ (0.15 mmol; M = Pt **1**, M = Pd **2**) was added. The reaction mixture was brought to room temperature within 3 h and then stirred for one more hour. The small excess of C₆F₅Li was destroyed by addition of ice-water (10 ml) at 0 °C. The organic layer was separated and the solvent was removed in vacuo. The product was recrystallized from CH₂Cl₂/hexane and dried under high vacuum.

4.6.1. [P]Pt(C₆F₅)₂ (**3h**)

White powder, dec. 129 °C, yield 101 mg (81%).

4.6.2. [P]Pd(C₆F₅)₂ (**4h**)

White powder, dec. 88 °C, yield 70 mg (63%).

4.7. Synthesis of $[P]PtFc_2$ (**3i**)

Solid $FcLi$ (230 mg, 1.2 mmol) was added to a solution of $[P]PtCl_2$ (**1**) (228 mg, 0.4 mmol) in toluene (20 ml) at $-10^\circ C$. The cooling bath was then removed and the mixture stirred for further 5 h at room temperature. After hydrolysis with water (20 ml) at $0^\circ C$, the organic layer was separated and brought to dryness in vacuo. Ferrocene was sublimed off from the red solid at $60^\circ C$ in a high vacuum. Recrystallization from CH_2Cl_2 /hexane and drying under high vacuum gave a red powder.

4.7.1. $[P]PtFc_2$ (**3i**)

Red powder, dec. $132^\circ C$, yield 236 mg (80%), 1H NMR ($CDCl_3$, $25^\circ C$): $\delta = 3.42$ (br, 3H, H^1), 3.90/4.27 (s/s, 5H/5H, $H^{cis/trans-Cp}$), 4.18/4.24 (m/m, 2H/2H, $H^{cis/trans-Fc}$), 4.32/4.42 (m/m, 2H/2H, $H^{cis/trans-Fc}$), 5.38 (m, 6H, $H^{2,7}$), 6.35 (m, 6H, $H^{3,6}$), 6.63 (m, 6H, $H^{4,5}$). $C_{41}H_{39}Fe_2PPt$, EI MS: m/e (%) = 370(27) [Fc_2^+], 304(66) [$(C_7H_7)_3^+$], 185(36) [Fc^+], 91(100) [$C_7H_7^+$].

4.8. Crystal structure analysis of $[P]Pt(C_6H_4-4-F)_2$ (**3g**)

The intensity data were collected on a STOE IPDS image plate system with Mo $K\alpha$ radiation ($\lambda = 71.073$ pm, graphite monochromator) at room temperature. The hydrogen atoms are in calculated positions. All non-hydrogen atoms were refined with anisotropic temperature factors. The hydrogen atoms were refined applying the riding model with fixed isotropic temperature factors.

4.8.1. $C_{33}H_{29}F_2PPt$ (**3g**)

Yellow prism of dimensions $0.35 \times 0.12 \times 0.08$ mm, crystallizes monoclinically, space group $P2_1/n$; $a = 1365.6(3)$, $b = 1459.7(3)$, $c = 1494.0(3)$ pm, $\beta = 109.52(3)^\circ$, $Z = 4$, $\mu = 5.089$ mm^{-1} ; 20750 reflections collected in the range $2-26^\circ$ in θ , 5042 reflections independent, 3785 reflections assigned to be observed ($I > 2\sigma(I)$); full matrix least-squares refinement with 334 parameters, R_1/wR_2 -values 0.041/0.095, absorption correction (numerical); max/min residual electron density $2.83/-1.03 \times 10^{-6}$ e pm^{-3} .

5. Supplementary information

Crystallographic data (excluding structure factors) for the structure reported in this paper have been deposited with the Cambridge Crystallographic Data Centre as supplementary publication CCDC No. 184030 (**3g**). Copies of the data can be obtained free of charge on application to The Director, CCDC, 12 Union Road, Cambridge CB2 1EZ, UK (fax: +44-1223-336033; e-

mail: deposit@ccdc.cam.ac.uk or www: <http://www.ccdc.cam.ac.uk>).

Acknowledgements

Support of this work by the Deutsche Forschungsgemeinschaft and the Fonds der Chemischen Industrie is gratefully acknowledged.

References

- [1] (a) M. Herberhold, *Metal π -Complexes; Vol. II: Complexes with Mono-Olefinic Ligands, Part 2, Specific Aspects*, Elsevier Scientific, Amsterdam, 1974; (b) L.B. Hunt, *Platinum Met. Rev.* 28 (1984) 76; (c) W. Siebert, G. Wilke, *J. Organomet. Chem.* 641 (2002) 1; (d) F.R. Hartley, *Chem. Rev.* 69 (1969) 799.
- [2] (a) C.A. McAuliffe, W. Levason, *Phosphine, Arsine and Stibine Complexes of the Transition Elements*, Elsevier, Amsterdam, 1979; (b) C.A. Tolman, *Chem. Rev.* 77 (1977) 313; (c) P.E. Garrou, *Chem. Rev.* 81 (1981) 229; (d) B. Chaudret, *Coord. Chem. Rev.* 86 (1988) 525; (e) S.J. Berners-Price, *Struct. Bonding* 70 (1989) 1.
- [3] (a) M.A. Bennett, H.W. Kouwenhoven, J. Lewis, R.S. Nyholm, *J. Chem. Soc.* (1964) 4570; (b) M.A. Bennett, W.R. Kneen, R.S. Nyholm, *Inorg. Chem.* 7 (1968) 556; (c) M.A. Bennett, W.R. Kneen, R.S. Nyholm, *J. Organomet. Chem.* 29 (1971) 293.
- [4] (a) P.W. Clark, J.L.S. Curtis, P.E. Garrou, G.E. Hartwell, *Can. J. Chem.* 52 (1974) 1714; (b) D.I. Hall, J.H. Ling, R.S. Nyholm, *Struct. Bonding* 15 (1973) 3; (c) H. Kurosawa, I. Ikeda, *J. Organomet. Chem.* 428 (1992) 289.
- [5] M. Herberhold, K. Bauer, W. Milius, *Z. Anorg. Allg. Chem.* 620 (1994) 2108.
- [6] M. Herberhold, T. Schmalz, W. Milius, B. Wrackmeyer, *Z. Anorg. Allg. Chem.* 628 (2002) 437.
- [7] M. Herberhold, T. Schmalz, W. Milius, B. Wrackmeyer, *Inorg. Chim. Acta* 334 (2002) 10.
- [8] M. Herberhold, T. Schmalz, W. Milius, B. Wrackmeyer, *Z. Naturforsch. B* 57 (2002) 53.
- [9] M. Herberhold, T. Schmalz, W. Milius, B. Wrackmeyer, *Z. Anorg. Allg. Chem.* 628 (2002) 971.
- [10] M. Herberhold, T. Schmalz, B. Wrackmeyer, *Z. Naturforsch. B* 57 (2002) 255.
- [11] M. Herberhold, T. Schmalz, W. Milius, B. Wrackmeyer, *J. Organomet. Chem.* 641 (2002) 173.
- [12] P.E. Garrou, G.E. Hartwell, *J. Organomet. Chem.* 71 (1974) 443.
- [13] (a) M.A. Alonso, J.A. Casares, P. Espinet, K. Soulantica, *Angew. Chem.* 111 (1999) 554; (b) M.A. Alonso, J.A. Casares, P. Espinet, K. Soulantica, *Angew. Chem., Int. Ed. Engl.* 38 (1999) 533.
- [14] J.A. Casares, P. Espinet, *Inorg. Chem.* 36 (1997) 5428.
- [15] (a) K.R. Dixon, in: J. Mason (Ed.), *Multinuclear NMR*, Plenum Press, New York, 1987, pp. 369–402; (b) P.S. Pregosin, R.W. Kunz, in: P. Diehl, E. Fluck, R. Kosfeld (Eds.), *NMR—Basic Principles and Progress*, vol. 16, Springer, Berlin, 1979.

- [16] W. McFarlane, *J. Chem. Soc. A* (1967) 1922.
- [17] (a) W. McFarlane, in: J.G. Verkade, L.D. Quin (Eds.), *Phosphorus-31 NMR Spectroscopy in Stereochemical Analysis*, VCH, Weinheim, 1987, pp. 115–150;
(b) W. McFarlane, *Annu. Rep. NMR Spectrosc.* 5A (1972) 353;
(c) W. McFarlane, D.S. Rycroft, *Annu. Rep. NMR Spectrosc.* 9 (1979) 319.
- [18] A. Bax, R. Freeman, *J. Magn. Reson.* 45 (1981) 177.
- [19] M.A. Bennett, R. Bramley, I.B. Tomkins, *J. Chem. Soc., Dalton Trans.* (1973) 166.
- [20] G.B. Deacon, E.A. Hilderbrand, E.R.T. Tiekink, *Z. Kristallogr.* 205 (1993) 340.
- [21] (a) J.A. Casares, P. Espinet, J.M. Martinez-Ilarduya, Y.-S. Lin, *Organometallics* 16 (1997) 770;
(b) T.J. Colacot, R.A. Teichman, R. Cea-Olivares, J.-G. Alvarado-Rodriguez, R.A. Toscano, W.J. Boyko, *J. Organomet. Chem.* 557 (1998) 169.
- [22] (a) F. Rebiere, O. Samuel, H.B. Kagan, *Tetrahedron Lett.* 31 (1990) 3121;
(b) D. Guillaneux, H.B. Kagan, *J. Org. Chem.* 60 (1995) 2502.